

A DISCRIMINATOR WITH DEEP LEARNING (RESNET-LST) FOR EVALUATING THE IMPACT OF URBAN MORPHOLOGICAL INDICATORS ON URBAN LAND SURFACE TEMPERATURES

ZISHEN BAI¹ and CHEN ZHANG²

¹University College London

²The University of Sheffield

¹zishen.bai.23@ucl.ac.uk, 0000-0002-8098-4729

²czhang120@sheffield.ac.uk, 0000-0001-7185-1054

Abstract. With global urban temperatures increasing yearly, city residents face serious health threats. Studies have shown a significant correlation between urban morphology and urban Land Surface Temperature (LST). However, the research findings of urban morphology and LST are frequently inconsistent or contradictory, which still need further exploration. The study proposes a ResNet-LST, which uses a Convolutional Neural Network (CNN) image classification model to link urban morphology with urban LST. The research aims to develop an effective real-time assessment tool for architects/urban designers to evaluate the impact of urban morphology indicators on urban LST. The ResNet-LST model went through 950 iterations with an overall accuracy of 79.48%. As a contribution, the study demonstrates that the surface temperature of each city region can reflect its contribution to the global temperature. Furthermore, the research results demonstrate the powerful flexibility in design decision-making for fast interaction using data-driven deep learning techniques. Designers will no longer need to pay high costs for LST simulations; image-based assessment models could give prompt feedback by recognizing 2D graphics of design proposals.

Keywords. LST, Urban form Indicators, Image Classification, Convolutional Neural Network, Open Urban Data.

1. Introduction

City residents face serious health threats with global urban temperatures rising each year. In China, approximately 831 million people live in cities. The Intergovernmental Panel on Climate Change (IPCC) states that for every 0.5 °C rise in average urban temperatures, an extra 27,900 people will die of heat-related illnesses (Seneviratne, 2022). The urban heat island effect was proposed by Lake Howard in 1883 when he observed a significant temperature increase in metropolitan areas compared to rural areas (Howard, 1883). Recent studies have focused on the complex effects of urban morphology, building materials, and land cover types on urban Land Surface Temperature (LST) (Mohamed et al., 2021). However, literature studies have shown

inconsistent and even contradictory effects of spatial morphological characteristics of cities on the urban thermal environment (Han, 2023). For example, research has shown that the Sky View Factor (SVF) positively correlates with LST. When the area of solar radiation increases, the surface temperature will increase (Daramola and Balogun, 2019). However, expanding building spacing may improve ventilation efficiency and reduce surface temperature (Yuan and Chen, 2011). Existing studies are still unclear about the relationship between urban morphology and surface temperature, which may be due to the coupling effect of urban spatial morphology on LST. Analyzing the influence of multiple factors on the thermal environment and prioritizing the influencing factors becomes challenging (Han, 2023). Recent studies are still trying to explain the urban LST development patterns and the prioritization of influencing factors with more advanced models (Siqi et al., 2023). It is worth noting that LST optimization guidance may have a limited contribution to early urban or architectural design proposals. The coupling effects of urban and LST remain unclear, and optimization guidelines for LST may not apply to the whole scenario (Du et al., 2022). Therefore, it is challenging to introduce LST optimization efforts in the early stages of urban/architectural design proposals. The study aims to develop an assessment tool for architects/urban designers to evaluate the urban LST level in the early proposal stage.

Research institutes have widely adopted LST modelling of satellite sensing data in urban form (Yin et al. 2018). The main idea of the research is to model the relationship between LST from satellite imaging and urban morphology features at the city scale via Convolutional Neural Network (CNN) learning. The research aims to allow designers to access their future LST trends by inputting a design proposal in a 2D layout format. The powerful computational capabilities of deep learning can save a significant amount of evaluation time for further proposal optimisation. More importantly, the study tests a hypothesis that the surface temperature of each urban area reflects its contribution to the global temperature, and the morphological indicators of the city can reflect the influence on LST.

A CNN image classification model based on the Res-Net algorithm is used in this study to develop a discriminator, ResNet-LST, to assess the potential LST of design proposals. A typical metropolitan area, Beijing city centre, was used as the study area. 4, 000 valid samples originating from the Beijing metropolitan area were used as the sample pool for ResNet-LST. The study samples are 2D images with HSV colour model, capturing building plan geometry, building heights, natural surface geometries and road morphology of Beijing city.

2. Methods and Materials

Figure 1 shows an overview of the workflow. The proposed modelling framework consists of three main components: (1) urban morphology data, (2) urban LST data, and (3) scene simulation with ResNet-LST. The challenge of the study is to create an adequate dataset (accuracy and resolution), which determines the credibility and stability of the output results.

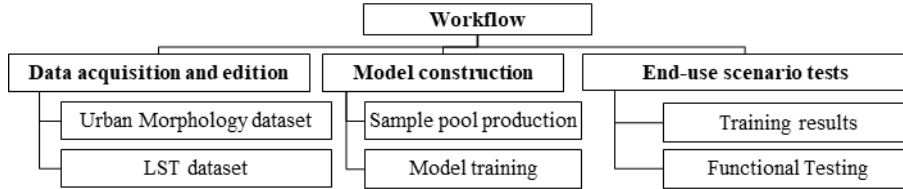


Figure 1. Workflow overview

2.1. URBAN MORPHOLOGY DATASET

In a broad sense, urban form is a complex system involving physical and non-physical forms (Skauge, 1995). The study is concerned with modelling urban physical form with LST, which follows the urban physical form indicators proposed by Jiang et al. in 2021 (1) texture (including volumetric ratio, texture density, mixed land use, and population density); and (2) spatial structure (including road density, connectivity, street accessibility, number and shape of land blocks, and compactness) (Jiang et al., 2021).

Amap (amap.com) provides a physical urban form data service, which contains vector data of buildings, natural surfaces, and roads in the city. ArcMap10.8 processes the urban form data and defines the geographic and projective coordinate systems: China Geodetic Coordinate System (CGCS) 2000 and Gauss-Krüger projection (Jekeli, 2006; Yang 2009). Urban morphology data editing aims to allow the CNN model to obtain a sample pool and to ensure that each sample is valid. After comparison, the study discarded the segmentation strategy with a low sample size ($N \leq 1,000$) and insufficient sample coverage ($S \leq 2,500 \text{ m}^2$). The size of the city samples used in this study is $400 \text{ m} \times 400 \text{ m}$. A total of 4,000 valid samples were generated.

2.2. LST DATASET

The LST data were collected from the Landsat 8 Collection 2 Level 2 of the United States Geological Survey (USGS) with a spatial resolution of 30 m (<http://www.usgs.gov/>). It is generally difficult for Landsat 8 to obtain time-adjacent clear-sky images with a 16-day revisit cycle. In order to reduce the interference of extreme weather (cloudy, extreme heat, and extreme cold) on the data, the study used the five-year mean values from 2018 to 2022 for the Beijing area (Zhu et al., 2022). For each image, the following tasks were done:

2.2.1. Electromagnetic Digital Number to Spectral Radiance Brightness

As thermal sensors could detect electromagnetic energy emitted above absolute zero (K), the received electromagnetic digital number could be converted into spectral radiance (Pal and Ziaul, 2017). Equation 1 demonstrates the conversion of image values to spectral radiance using the conversion equation (Chander and Groeneveld 2009).

$$L_{\lambda} = \frac{(L_{\max\lambda} - L_{\min})}{(Q_{\text{Calmax}} - Q_{\text{Calmin}})} * Q_{\text{Cal}} + L_{\min\lambda} \quad (1)$$

Where $Q_{\text{Calmin}}=0$, $Q_{\text{Calmax}}=255$ and $Q_{\text{Cal}}=\text{number of each pixel}$. $L_{\min\lambda}$ and $L_{\max\lambda}$ are the spectral weakest and strongest radiant luminance at numbers 0 and 255 (Soltanifard and Aliabadi, 2019).

2.2.2. Spectral radiation brightness converted to brightness temperature

Equation 2 presents the approach to obtain the brightness temperature.

$$T_b = \frac{k_2}{L_{\lambda} \left(\frac{k_1}{L_{\lambda}} + 1 \right)} \quad (2)$$

Where $T_b = \text{brightness temperature (K)}$, $L_{\lambda} = \text{spectral radiant brightness in } Wm^{-2}sr^{-1}\mu m^{-1}$, and K_1 and K_2 are two pre-emission calibration constants.

2.2.3. Obtaining LST raw

Since brightness temperature is a reference value, LST30m needs to be converted based on the land cover factor. Equation 3 follows the methodology proposed by Artis and Carnahan in 1982 to calculate LST (Artis and Carnahan, 1982).

$$LST_{\text{raw}} = \frac{T_b}{1 + \left(\lambda * \frac{T_b}{\alpha} \right) L_n(\epsilon)} \quad (3)$$

Where LST raw is based on the surface temperature obtained from Landsat 8 product at 30m resolution, $\lambda=11.5 \mu m$, $T_b = \text{brightness temperature}$, $\alpha=1.38*10^{-23}J/K$, $\epsilon = \text{ranges between 0.97 and 0.99}$ (Pal and Ziaul, 2017).

2.2.4. Acquire the sample mean LSTWA

For modelling urban morphology with LST within medium-scale urban areas, each sample needs to be assigned a unique LSTWA. Equation 4 is a weighted average approach to obtain LST values within each sample area.

$$LST_{WA} = \frac{\sum(LST_{\text{raw}} \times S_{\text{raw}})}{S_{\text{area}}} \quad (4)$$

Where S_{raw} is the area occupied by each LST raw value in the study area, $S_{\text{area}}=160,000 \text{ m}^2$.

2.3. SAMPLE POOL PRODUCTION

CNN is a supervised learning image recognition/classification model that uses spectral features obtained from training samples to classify input images (urban morphology features) (Das, 2017). Before training, the study did the following editing of the raw urban morphology data:

2.3.1. Image tagging

The vector values provided by Amap are required to be converted into images for CNN to read the spectral features. The conversion was done in ArcMap 10.8, and three

colour layers were used to define the urban morphology. Figure 2 shows the tagged sample images based on the Hexcone model in the RGB colour system. The pink area shows the building heights based on the three-metre gradient tags in the study area. Roads are black, and natural surfaces are green, reflecting the pavement density, road network density and natural surface density of the study area.



Figure 2: Map of urban morphology after tagging

2.3.2. Sample group classification

According to the distribution pattern of LSTWA values in Beijing, five value intervals were calculated and obtained by the natural breakpoint method (Figure 3). Among 4,000 valid samples, the lowest value of LSTWA in Beijing was collected as 5.6533°C, and the highest was 43.4640°C. The minimum sample interval was (5.6533, 22.9793), and 25 samples were collected. The maximum sample interval was centred on (34.1673, 36.0673), and 1, 616 samples were collected.

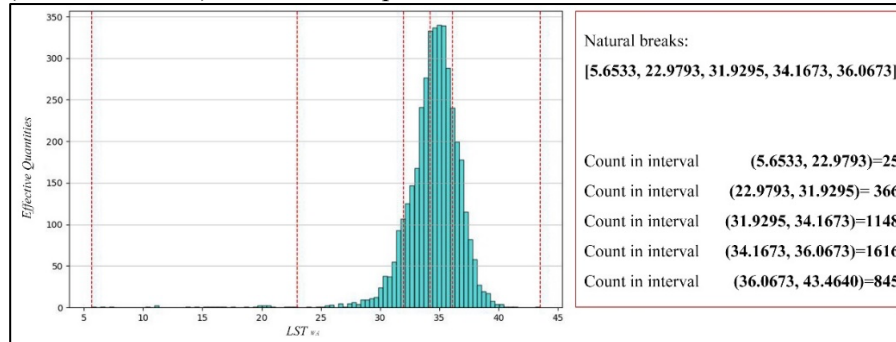


Figure 3: Natural Breakpoint Analysis for LSTWA

2.3.3. Sample Printing

Study of a script written in the Python3 language for efficient printing maps in ArcMap 10.8 as JPEG images. The core module of the script uses the Search-Cursor function in ArcMap 10.8.1, which creates read-only cursors on element categories or tables. The Search-Cursor function allows clauses or fields to restrict the query and sort the results (Tateosian, 2015). The sample pool of the supervised learning model requires setting the sample categories before training, which is determined by the natural breakpoint

distribution according to the LSTWA. In the script, the syntax if for LSTWA is used for the output path programming. The ExportToJPEG function in the Arcpy module sets the size and resolution for the output samples. The script outputs the images from ArcMap 10.8.1 as JPEG files and stores them in five folders created according to the range of LSTWA values of the area where the samples are located. A total of 4,000 valid samples were generated.

2.4. MODEL TRAINING

EasyDL is an AI service development platform provided by Baidu Brain (<https://ai.baidu.com/easydl/>) with deployable machine learning algorithms (Singh, 2016). The Deep Residual Learning algorithm which used in this study, won the best performance award in the 2015 ILSVRC computer vision competition (He et al.). Baidu Brain provides a powerful arithmetic platform, and this study used a remote online service platform. The basic parameters of the model training server were Tesla P40, Video Mem: 24GB, CPU: 12 Cores, RAM: 40G.

To prevent excessive variation in the number of samples, 25 samples in the minimum sample interval (5.6533, 22.9793) were discarded. The study proposes a method for evaluating the contribution of regional temperature to global LST based on the median and mean of LSTWA values. Negative represents that the urban form of the study area can be used to reduce urban LST, and Positive represents that it may potentially enhance LST. Based on the principle of contribution, the study defines the sample group (31.9295, 34.1673) that contributes to the global LST with a primary negative effect, named Negative_Lv01; samples in the interval (22.9793, 31.9295) have a secondary negative effect on the global LST, named Negative_Lv02; furthermore, the sample groups (34.1673, 36.0673) and (36.0673, 43.4640) have a LST improvement had a propulsive effect, named Positive_Lv01 and Positive_Lv02, respectively.

In the urban morphology samples, a colour gradient system was used for different urban morphology indicators, which means the distortions or colour changes may mislead the training model. Therefore, randomly occurring XY translations (Translate_X; Translate_Y) were used in the incremental training strategy with a probability of 10%. (Figure 4)

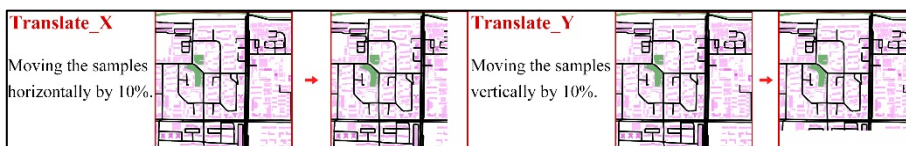


Figure 4. XY translations

3. Results and Functional Testing

3.1. TRAINING RESULTS

During the model training process, invalid samples negatively affected the training results. After data cleaning, 186 invalid samples were removed, and 25 samples within (5.6533, 22.9793) were discarded, leaving a sample pool 3,789. A randomly taken

sample pool of 70% (2,650) samples was used for the training set, and 1,139 (30%) samples were used for the test set. After 28.5 hours of training, the model went through 950 iterations and achieved a combined accuracy of 79.48%.

3.2. USER HANDBOOK

The handbook aims to explain the research methodologies in practical design work with the user handbook. The assessment tool is also a way for designers better to understand the relationship between urban form and LST. Specifically, the user handbook contains the following key points:

3.2.1. *Provide a guideline for using Resnet-LST.*

Designers need to produce a 2D draft of their proposal. A square boundary line with sides of 400 metres is required and the assessment area is only allowed to be filled in within the boundary line. If the study area exceeds the boundary line, consider splitting the proposal into multiple samples.

The second step in sample production was to create labels for the samples based on the colour cards. Figure 2 lists the colour reference sheets for the features labelled. The colour reference table includes building heights, terrain heights, natural surfaces, and roads. Before submitting for assessment, the sample files need to be printed. Typically, a print ratio of 1:2000 and an image resolution of 300 for JPEG format files is recommended.

3.2.2. *Sample Submission and Understanding the Results*

The classification categories permitted by the Resnet-LST model depend on the parameters during the model training period. In other words, the input sample group categories determine the range of samples that can be recognised and output by the model. The Resnet-LST model will output the possible probability of each sample group, with the highest probability sample group indicated as the most tendentious. After testing, the two groups with the highest predicted probabilities output by the Resnet-LST model generally span two adjacent sample bands, which means that a suggested direction is provided for scenario optimisation.

3.3. FUNCTIONAL TESTING

A social housing project was selected for the study to demonstrate that the trained ResNets-LST predictor could output valid results. The Baiziwan social housing project is located on the 4th ring road in the centre of Beijing (39.89°N, 116.51°E) and was completed by MAD Studio in 2021 (Iype, 2021). The study used ResNets-LST to assess the LST changes in Baiziwan social housing during the construction cycle. Specifically, the scenario testing tasks are as follows:

3.3.1. *Find a test target and launch the model*

The Baiziwan social housing project is located within the study area (Sample ID = 66), with the same urban context (economic, population, industry, climate) as the sample

pool for this training. The initial LSTWA = 32.78°C, which is within the (36.0673, 43.4640) sample set, positively enhances the city's global LST and belongs to the Positive_Lv02 level. Before the retrofit, the study area had a high density of low-rise buildings and scarce vegetation, which negatively affected heat evacuation (Chen et al. 2023).

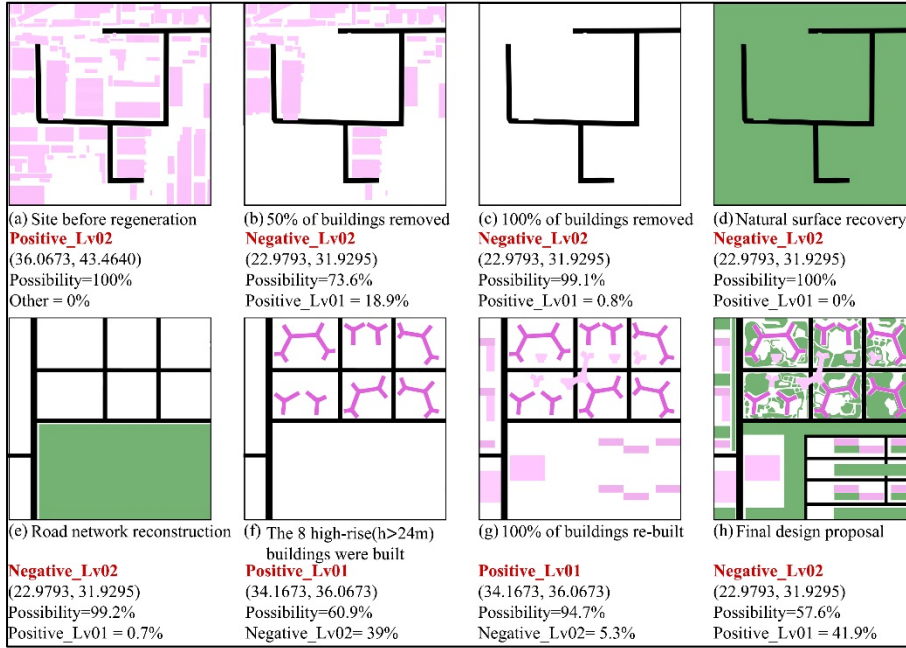


Figure 5. ResNets-LST shows the results of the project construction cycle prediction.

3.3.2. Explanation

In the test results, the first significant change in the predicted values was after 50% of the buildings were removed (refer to b in Figure 5), with a 73.6% probability that LSTWA was at Negative_Lv02 (22.9793, 31.9295). The large area of unused space replaces the high density of buildings on the site, which potentially increases wind speed and thus accelerates heat losses (Yuan and Chen, 2011). The results of subsequent tests confirmed this conjecture, with the probability of predicting the LSTWA to be at Negative_Lv02 increasing to 99.2% after all the buildings were removed and the natural surface restored.

The second significant change in the predicted values occurred after the site was recovered with buildings (refer to g in Figure 5), where the predictor showed that there existed a 94.7% probability that the LSTWA was at Positive_Lv01 (34.1673, 36.0673). The predictor also reasonably explains the relationship between building form and LST. Specifically, after eight high-rise buildings ($h > 24\text{m}$) are constructed (refer to f in Figure 5), the predicted probability that the LSTWA is at Positive_Lv01 is 60.9%. However, along with the low-rise buildings, the predicted probability of Positive_Lv01 was raised to 94.7% (refer to g in Figure 5). Building height shows a negative

correlation with LST, and the "tall-slim" building form may benefit the temperature dissipation at the surface (Chen et al., 2022). Furthermore, the role of vegetation cannot be ignored. The predictor suggests a site filled with vegetation will lower the surface LST with a 57.6% probability of being in Negative_Lv02 (refer to h in Figure 5).

In summary, ResNets-LST demonstrates how LST changes during the process of urban morphological transformation and that the changes are consistent with the interpretation of LST trends in the existing literature.

4. Conclusion and further work

This study presents ResNets-LST, an urban surface temperature modelling tool using image classification techniques, for rapid assessment of the influence of urban morphology in LST. The study demonstrated that the surface temperature of each city region can reflect its contribution to the global temperature. Thus, the city morphology metrics can explain its influence on LST. Using data-driven deep learning methods can provide the flexibility to interact with design decisions quickly.

However, there is still a need for further research on ResNets-LST as a prototype. Firstly, the ResNets-LST predictor is location-based, which can only be applied to the training area. In the future, research needs to test the ability of ResNets-LST to generalise to different urban contexts. Secondly, the sample pool still needs to provide sufficient evidence for its validity. Research still needs to develop a more robust sample selection and cleaning methodology to ensure more reasonable outputs.

Image recognition technology effectively saves testing time, which opens the possibility of developing more automated frameworks in the future. ResNets-LST can be engaged as a discriminator for Generative Adversarial Networks to train pix2pix models (GAN pix2pix) to build Generative Multi-Objective Optimisation frameworks (GMOO). Generative AI for interaction design or machine learning-assisted design will bring a new dawn to the architecture/urban design field.

References

- Artis, D. A., & Carnahan, W. H. (1982). Survey of emissivity variability in thermography of urban areas. *Remote sensing of Environment*, 12(4), 313-329. [https://doi.org/10.1016/0034-4257\(82\)90043-8](https://doi.org/10.1016/0034-4257(82)90043-8).
- Chander, G., & Groeneveld, D. P. (2009). Intra-annual NDVI validation of the Landsat 5 TM radiometric calibration. *International Journal of Remote Sensing*, 30(6), 1621-1628. <https://doi.org/10.1080/01431160802524545>.
- Chen, C., Bagan, H., Yoshida, T., Borjigin, H., & Gao, J. (2022). Quantitative analysis of the building-level relationship between building form and land surface temperature using airborne LiDAR and thermal infrared data. *Urban Climate*, 45, 101248. <https://doi.org/10.1016/j.uclim.2022.101248>.
- Chen, W., Zhang, J., Liu, S., Liang, S., Zhang, Y., & Fu, S. (2023). The spatial configuration of buildings: A vital consideration impossible to ignore in regulating urban land surface temperature? Evidence from 35 Chinese cities. *Science of The Total Environment*, 865, 160946. <https://doi.org/10.1016/j.scitotenv.2022.160946>.
- Daramola, M. T., & Balogun, I. A. (2019). Analysis of the urban surface thermal condition based on sky-view factor and vegetation cover. *Remote Sensing Applications: Society and Environment*, 15, 100253. <https://doi.org/10.1016/j.rsase.2019.100253>.

- Das, T. (2017). Machine Learning algorithms for Image Classification of hand digits and face recognition dataset. *Machine Learning*, 4(12), 640-649.
- Du, S., Zhang, X., Jin, X., Zhou, X., & Shi, X. (2022). A review of multi-scale modelling, assessment, and improvement methods of the urban thermal and wind environment. *Building and Environment*, 213, 108860. <https://doi.org/10.1016/j.buildenv.2022.108860>.
- Han, W. (2023). Analyzing the scale dependent effect of urban building morphology on land surface temperature using random forest algorithm. *Scientific Reports*, 13(1), 19312. <https://doi.org/10.1038/s41598-023-46437-w>.
- He, K., Zhang, X., Ren, S., & Sun, J. Deep residual learning for image recognition (2015). cite. *arXiv preprint arxiv:1512.03385*. <https://doi.org/10.1109/CVPR.2016.90>.
- Iype, J (2021) *MAD's first social housing project Baiziwan integrates community into urban fabric*. Retrieved August 2022, from <https://www.stirworld.com/see-features-mad-s-first-social-housing-project-baiziwan-integrates-community-into-urban-fabric/>.
- Jekeli, C. (2006). *Geometric reference systems in geodesy*. Division of Geodesy and Geospatial Science, School of Earth Sciences, Ohio State University, 25.
- Jiang, Z., Cheng, H., Zhang, P., & Kang, T. (2021). Influence of urban morphological parameters on the distribution and diffusion of air pollutants: A case study in China. *Journal of Environmental Sciences*, 105, 163-172. <https://doi.org/10.1016/j.jes.2020.12.035>.
- Pal, S., & Ziaul, S. K. (2017). Detection of land use and land cover change and land surface temperature in English Bazar urban centre. *The Egyptian Journal of Remote Sensing and Space Science*, 20(1), 125-145. <https://doi.org/10.1016/j.ejrs.2016.11.003>.
- Seneviratne, S. (2022). Weather and climate extreme events in a changing climate. In *IPCC Sixth Assessment Report* (pp. 1513–1766). <https://doi.org/10.1017/9781009157896.013>.
- Singh, J. (2016). Baidu unveils open-source deep learning platform PaddlePaddle. *Open Source for You*.
- Siqi, J., Yuhong, W., Ling, C., & Xiaowen, B. (2023). A novel approach to estimating urban land surface temperature by the combination of geographically weighted regression and deep neural network models. *Urban Climate*, 47, 101390. <https://doi.org/10.1016/j.uclim.2022.101390>.
- Skauge, J. (1995). Urban design analysis by computer. *Cities*, 12(6), 425-430. [https://doi.org/10.1016/0264-2751\(95\)00089-5](https://doi.org/10.1016/0264-2751(95)00089-5).
- Soltanifard, H., & Aliabadi, K. (2019). Impact of urban spatial configuration on land surface temperature and urban heat islands: A case study of Mashhad, Iran. *Theoretical and applied climatology*, 137, 2889-2903. <https://doi.org/10.1007/s00704-018-2738-4>.
- Tateosian, L. (2015). *Reading and Writing with Cursors*. Python For ArcGIS, 309-333.
- Yang, Y. (2009). *Chinese geodetic coordinate system 2000*. Chinese Science Bulletin, 54(15), 2714-2721.
- Yin, C., Yuan, M., Lu, Y., Huang, Y., & Liu, Y. (2018). Effects of urban form on the urban heat island effect based on spatial regression model. *Science of the Total Environment*, 634, 696-704. <https://doi.org/10.1016/j.scitotenv.2018.03.350>.
- Yuan, C., & Chen, L. (2011). Mitigating urban heat island effects in high-density cities based on sky view factor and urban morphological understanding: a study of Hong Kong. *Architectural Science Review*, 54(4), 305-315. <https://doi.org/10.1080/00038628.2011.613644>.
- Zhu, X., Duan, S. B., Li, Z. L., Wu, P., Wu, H., Zhao, W., & Qian, Y. (2022). Reconstruction of land surface temperature under cloudy conditions from Landsat 8 data using annual temperature cycle model. *Remote Sensing of Environment*, 281, 113261. <https://doi.org/10.1016/j.rse.2022.113261>.